AJNR

Experimental Model of Dissecting Aneurysms

Takeshi Okamoto, Shigeru Miyachi, Makoto Negoro, Goro Otsuka, Osamu Suzuki, Hiroomi Keino and Jun Yoshida

AJNR Am J Neuroradiol 2002, 23 (4) 577-584
http://www.ajnr.org/content/23/4/577

AJNR Am J Neuroradiol 23:577–584, April 2002

Experimental Model of Dissecting Aneurysms

Takeshi Okamoto, Shigeru Miyachi, Makoto Negoro, Goro Otsuka, Osamu Suzuki, Hiroomi Keino, and Jun Yoshida

BACKGROUND AND PURPOSE: **The pathogenesis and optimal treatment for arterial dissection are still unclear. We devised an experimental model of arterial dissection and observed the morphologic changes with angiography.**

METHODS: **Sixty-four experimental dissections were created in the common carotid arteries of 34 mongrel dogs. After a small incision was made in the arterial adventitia, it was dissected from the media. Elliptical defects (2, 4, 6, and 8 mm in groups I-A, I-B, I-C, and I-D, respectively; n = 47) or longitudinal incisions (4, 6, and 8 mm in groups II-A, II-B, and II-C, respectively; n = 17) were made in the intima distal to the adventitial incision to serve as an entry zone for dissection.**

RESULTS: **Immediately after the lesions were created, the influx of blood into the dissected cavity produced massive subadventitial hematomas, resulting in stenotic changes in all of the arteries, including seven with occlusion. Follow-up (1-week) angiograms demonstrated complete healing, with normal arterial calibers in 11 (79%) of 14 I-A lesions and aneurysm formation in nine (69%) of 13 I-B lesions. All 10 I-D lesions had complete arterial occlusion. Persistent stenosis was observed in all 10 I-C lesions; six of these developed aneurysms. Pathologic examination of the freshly dissected cavities revealed a clot-filled cleft between the media and adventitia. Mature aneurysms, evaluated 3 mo later, had endothelialization within the aneurysmal dome.**

CONCLUSION: **Morphologic changes after arterial dissection are closely related to the size of the intimal entry zone, which may determine whether a dissecting aneurysm forms.**

Arterial dissection can be caused by external forces due to trauma (eg, penetrating or blunt injury); by intraluminal lesions due to atherosclerotic, dysplastic, or infectious processes; or by iatrogenic intimal trauma during catheterization (1–8). Even individuals with no apparent risk factors can have cerebral arterial dissection, which causes severe pain with or without a neurologic deficit. Although such idiopathic arterial dissections have high morbidity rates, the pathogenesis and the optimal treatment strategy are still unclear. Further, arterial dissection can have one of two clinical patterns, or both: dissecting aneurysm with hemorrhage and stenosis or occlusion with ischemic symptoms (9). However, the factors that define the morphologic and clinical characteristics of dissection are undetermined. Therefore, we developed a canine model of arterial dissection and observed the morphologic changes at serial angiography and histopathologic examination to clarify the causes and mechanisms of dissecting aneurysm formation and arterial occlusion.

Received April 27, 2001; accepted after revision October 8.

From the Department of Neurosurgery, Nagoya University Graduate School of Medicine, Japan (T.O., S.M., M.N., G.O., O.S., J.Y.), and the Department of Perinatology, Institute of Developmental Research, Aichi, Japan (H.K.).

Address reprint requests to Takeshi Okamoto, MD, Department of Neurosurgery, Nagoya University Graduate School of Medicine, 65 Tsurumai-cho, Showa-ku, Nagoya, 466-8550 Japan.

Methods

Thirty-four mongrel dogs (weight, 16–20 kg) were used for this study, which was performed by using a protocol approved by the Nagoya University Animal Care Committee. The animals were anesthetized with an intramuscular injection of ketamine hydrochloride (3 mg/kg) and with an intravenous injection of pentobarbital (5 mg/kg). Then, they were intubated and allowed to spontaneously breathe room air. General anesthesia was maintained with additional doses of pentobarbital, as required. Each surgical procedure was performed under sterile conditions with the aid of a surgical microscope.

With the dogs in the supine position, a longitudinal paramedian skin incision, about 10 cm long, was made in the anterior aspect of the neck adjacent to the sternocleidomastoid muscle, and the common carotid artery (CCA) was isolated. After vascular clamps were placed distally and proximally, a small incision, limited to the adventitia, was made. Then, the adventitia was dissected from the media. After the two layers were sufficiently dissected, various longitudinally oriented elliptical defects or longitudinal incision were made in the intima, including the media. These steps were meticulously performed by using small scissors inserted through the adventitial window. The intimal defect (entry zone) was created at a point distal to the adventitial incision to ensure that the adventitia remained

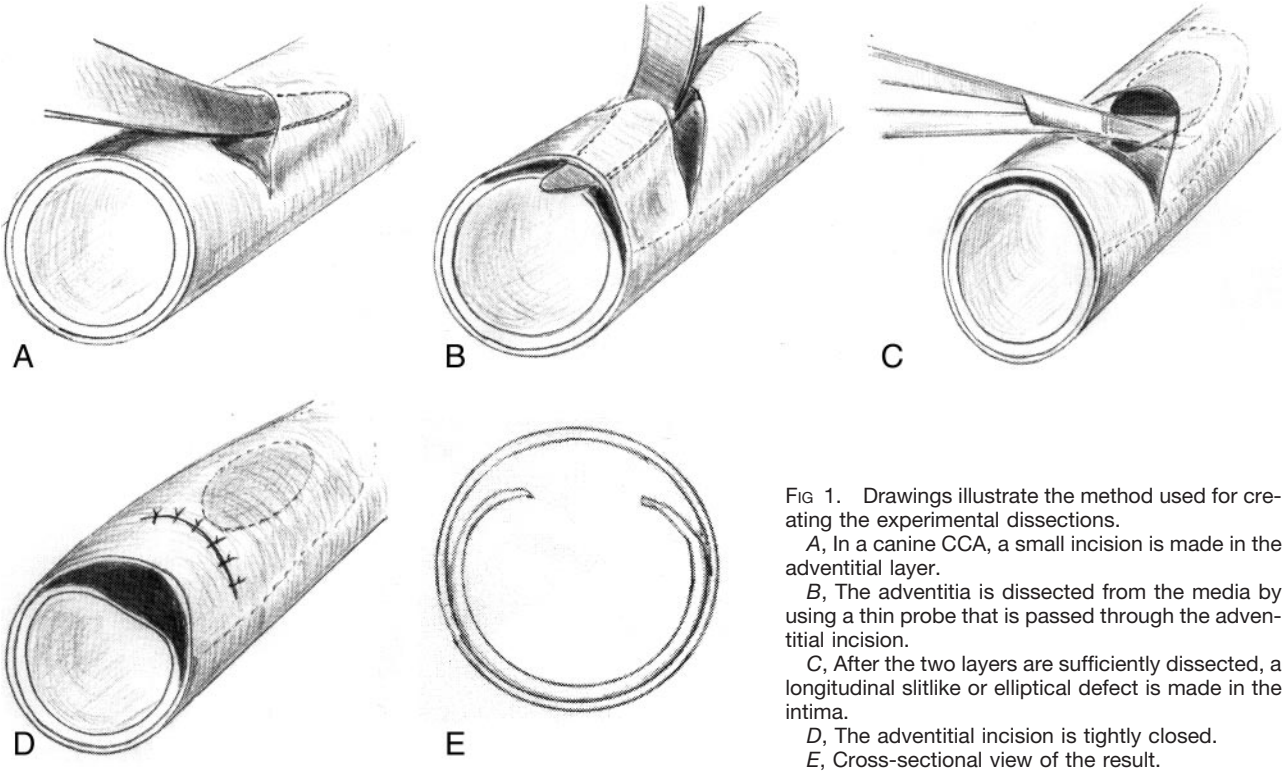

FIG 1. Drawings illustrate the method used for creating the experimental dissections.

A, In a canine CCA, a small incision is made in the adventitial layer.

B, The adventitia is dissected from the media by using a thin probe that is passed through the adventitial incision.

C, After the two layers are sufficiently dissected, a longitudinal slitlike or elliptical defect is made in the intima.

D, The adventitial incision is tightly closed.

E, Cross-sectional view of the result.

Summary of angiographic changes

Group*	Normal	Aneurysm	Aneurysm and Stenosis	Stenosis	Occlusion	No Follow-Up	Total
I-A	0/11/13	0/1/0	0/0/0	14/2/0	0/0/0	0/0/1	14
I-B	0/3/7	0/8/6	0/1/0	12/1/0	1/0/0	0/0/0	13
I-C	0/0/2	0/0/0	3/6/2	5/4/4	2/0/0	0/0/2	10
I-D	0/0/0	0/0/0	3/0/0	5/0/0	2/10/10	0/0/0	10
II-A	0/5/6	0/2/1	0/0/0	7/0/0	0/0/0	0/0/0	7
II-B	0/3/3	0/1/1	0/1/0	5/0/0	0/0/0	0/0/1	5
II-C	0/0/2	0/1/0	0/3/2	3/1/1	2/0/0	0/0/0	5

Note.—Data are the number of changes at the acute/subacute/chronic stages.

* Elliptical lesions were made with a 2-, 4-, 6-, and 8-mm incisions in groups I-A, I-B, I-C, I-D, respectively. Longitudinal lesions were made with a 4-, 6-, and 8-mm incisions in groups II-A, II-B, and II-C, respectively.

intact where blood entered the dissected cavity. After the presence of communication between the subadventitial space and the vessel lumen was confirmed, only the adventitial layer was tightly closed by using an 8–0 nylon suture. Both clamps then were released from the CCA. Oozing from the incised segment of adventitia was controlled with gentle manual compression and by coating the adventitia with microfibrillar collagen powder (Fig 1).

Sixty-four artificial dissections were made in one or both carotid arteries. In 47 dissections, an elliptical intimal entry zone. These elliptical lesions had longitudinal lengths of 2–8 mm: Fourteen lesions were made with a 2-mm incision (group I-A); 13, with a 4-mm incision (I-B); 10, with a 6-mm incision (I-C); and 10, with an 8-mm incision (I-D). In 17 dissections, the intima was cut longitudinally. These incisions were 4–8 mm long: Seven lesions were made with a 4-mm incision (group II-A); five, with a 6-mm incision (II-B); and five, with an 8-mm incision (II-C) (Table). The width of the ellipses was equal to half the arterial diameter, which was approximately 2 mm. The length of the incision was measured exactly and confirmed by using a scale.

Immediately after these procedures were completed, external changes in the dissected portion were observed macroscopically. Then, carotid angiogram was performed by using the Seldinger method. In all cases, a second angiogram was obtained 30 minutes to 2 hours after the initial angiogram to evaluate acute changes, including improvement in the stenosis, progressive occlusion, and recanalization. In all cases, 1-week follow-up angiography was performed, and 60 lesions were examined at follow-up angiography 3 months later. No anticoagulation or antiplatelet medication was administered before, during, or after creation of the dissections.

After final follow-up angiography or after an animal's death from complications, dissected arteries were harvested for histopathologic examination. The specimens were divided into two pieces. One was processed for observation of luminal changes at light microscopy, and the other was processed for evaluation of the endothelialization of the dissected site at scanning electron microscopy (SEM). Statistical analysis among the groups defined by incision size and shape was performed by using the Fisher exact probability test.

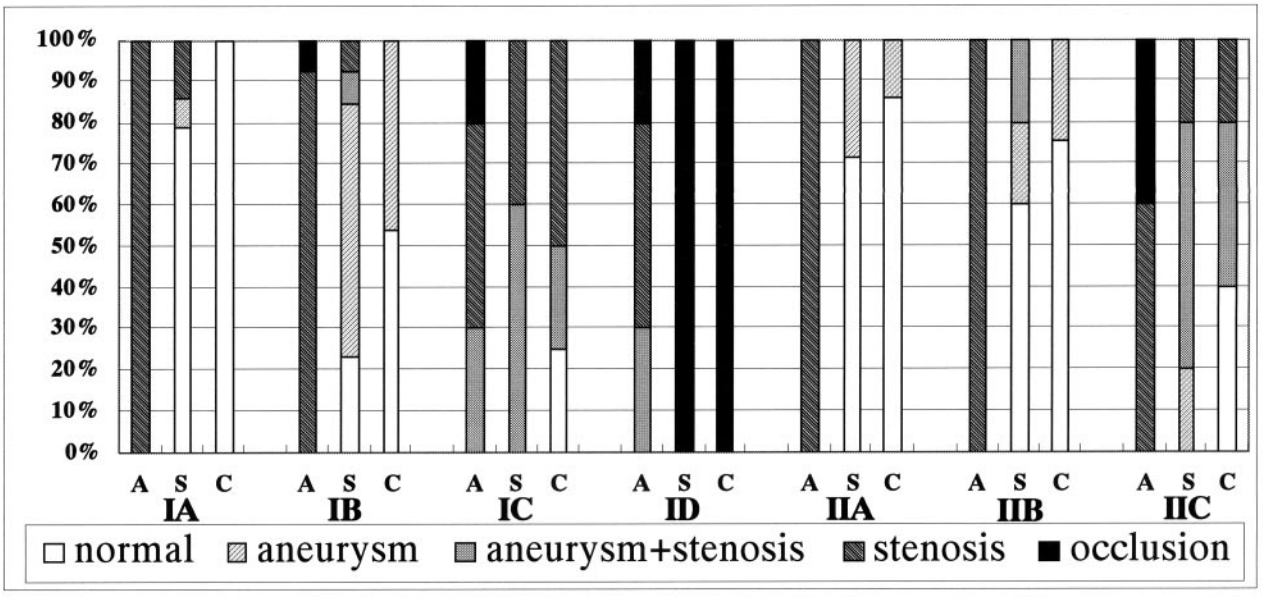

FIG 2. Bar graph summaries the serial angiographic changes. *A* indicates the acute stage; *C*, chronic stage; *S*, subacute stage.

Results

Results are summarized in the Table and Figure 2.

Acute Morphologic Change

In all, 64 artificial dissections were successfully completed. Immediately after recanalization, all lesions showed abrupt formation of a dense subadventitial hematoma due to influx of blood through the intimal entry zone (Figs 3–5). Usually, these were massive and frequently extended distally and also proximally from the intimal entry zone along the plane of adventitial separation. The initial angiogram demonstrated stenotic change in the artery in all lesions, including total occlusion in seven (Fig 5). The stenotic change was particularly marked at the site of the intimal entry zone. Occasionally, the stenosis extended over a long segment, representing expansion of the subadventitial hematoma (Fig 5). In 40 lesions, a subadventitial pseudolumen was visualized; it showed an influx of the contrast medium (Figs 3, 4). When we compared the groups according to characteristics of the intimal entry zone, severe stenotic changes most often were found in groups I-C and I-D. Compared with groups with elliptical lesions, groups with longitudinal incisions had less extensive subadventitial hematoma formation . In all cases, the second angiogram was obtained in the acute stage within 2 hours after the initial one. As for external appearance in this stage, swelling was noted, and the reddish subadventitial hematoma was darkened where it extended far from the intimal entry zone. No pseudolumen was opacified on angiograms obtained at 2 hours. Of seven lesions with total occlusion of the artery, as depicted on the initial angiogram, images of six showed recanalization. Forty-nine of 57 lesions with initial stenosis improved on the second angiogram obtained 30 minutes to 2 hours after the initial angiogram. Particularly, lesions with small entry zones (I-A, I-B, II-A) tended to have marked improvement.

Subacute Morphologic Change

All animals underwent follow-up angiography at 1 wk. Angiograms obtained at this subacute stage demonstrated morphologic changes that varied with the size of the intimal entry zone. In 11 (79%) of 14 lesions in group I-A, the stenosis had normalized, and the arterial contour was smooth. However, lesions in group I-B (n = 13) resulted in aneurysm formation in eight lesions (62%); an aneurysm with stenosis was present in one, and persistent stenosis without aneurysm was present in one. In the 10 lesions in group I-C, all showed persistent stenosis (Fig 4), and six were associated with an aneurysm (Fig 3). All lesions in group I-D (n = 10) were associated with complete occlusion of the artery (Fig 5). As for the groups with longitudinal incisions (II-A, II-B, II-C) no notable relationship was found between the length of the incision and morphologic change (Table, Fig 2). Aneurysms were berry-shaped and limited to the area of the intimal entry zone (Fig 3).

Chronic Morphologic Change

Sixty lesions were followed up for 3 months. One dog died because of systemic complications, and three died within 2 weeks because of repeated rupture of aneurysms. Postmortem histopathologic study showed that all were pseudoaneurysms and that the rupture points were at the top of the aneurysms, not at the site of surgical access. These cases were in groups I-B, I-C, and II-C. In lesions with aneurysms, the aneurysms were unchanged in size or slightly smaller (Fig 3); no aneurysm enlarged. In 10 of 19 cases, persistent stenosis observed in the subacute stage recovered well, particu-

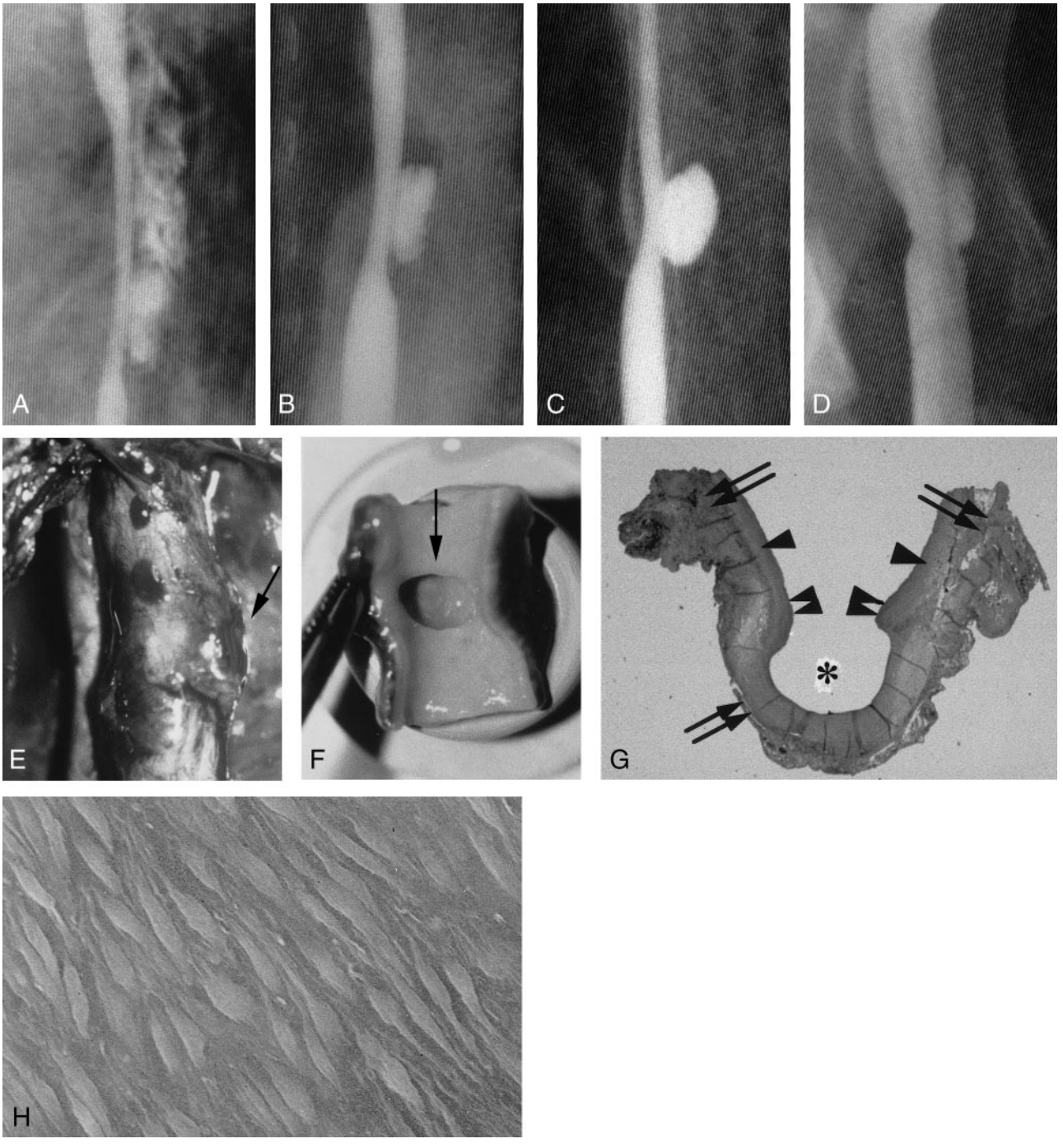

FIG 3. Example of aneurysm formation, with persistent stenosis (group I-C 6-mm elliptical defect).
A, Angiogram shows a double shadow due to a massive adventitial hematoma that formed immediately after lesion creation.
B, Angiogram obtained 2 hours later shows a subadventitial hematoma with the characteristics of an aneurysmal pouch.
C, Angiogram obtained 1 week later shows that the hematoma has become a saccular aneurysm.
D, Chronic-stage (3-month) angiogram shows that the aneurysm is smaller.
E, Photograph shows external protrusion of the aneurysm (*arrow*).
F, Chronic-stage photograph obtained in shows that part of the intimal defect extends to the aneurysm orifice (*arrow*).
G, Chronic-stage photomicrograph shows that the inner layer of the aneurysm dome (*asterisk*) is covered with organized clots and fully endothelialized (elastica van Gieson stain, original magnification ×5). *Arrows* indicate the adventitia; *single arrowheads*, media; *double arrowheads*, intima.
H, Scanning electron micrograph shows endothelialization (original magnification ×700).

larly in the lesions with a small entry zone (I-A, I-B, II-A). No complete occlusion recanalized. Only three lesions ruptured; all had pseudoaneurysms in the subacute stage. Macroscopically, the swollen contours of the arteries with an aneurysm persisted, and the aneurysm domes became firmer. Extensive subadventitial hematomas still appeared black, but the width of the artery had become essentially normal.

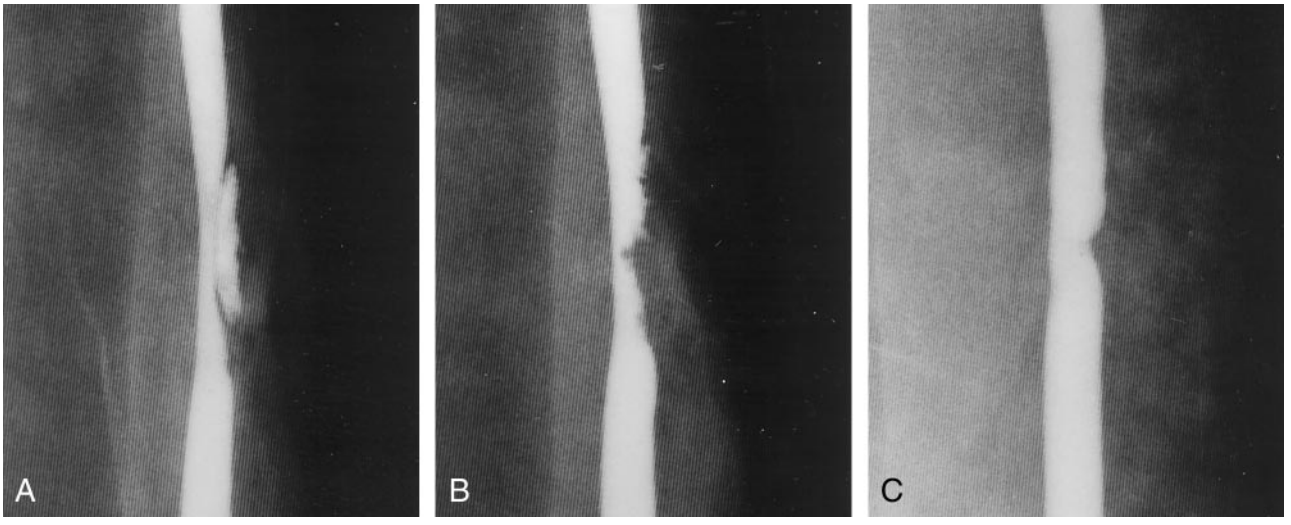

FIG 4. Example of persistent stenosis (group I-C 6-mm elliptical defect).
A, Angiogram obtained just after lesion creation shows a subadventitial hematoma that is compressing the arterial lumen.
B, Angiogram obtained 2 hours later shows that the subadventitial hematoma has spontaneously thrombosed, but it is still compressing the arterial lumen.
C, Angiogram obtained in the chronic stage shows that the stenosis has improved.

Histopathologic Change

On transverse cross sections, the dissection cavity was microscopically evident as a crescent-shaped cleft between the adventitia and media that was filled with a fresh clot in the acute stage. Examination of ruptured pseudoaneurysms revealed extraadventitial cavity formation that extended from the tear in the adventitia at the top of the aneurysm; the cavity was covered with a thin fibrin membrane. Serial sections indicated that the clots extended both distally and proximally to the intimal entry zone. In lesions with persistent stenosis, subadventitial clots were partially organized in the chronic stage (Fig 5). In lesions with aneurysm formation, a portion of the intimal entry zone extended to the orifice of the aneurysm. In cases of aneurysm with stenosis, external protrusion of the aneurysm was small, and clots in the surrounding subadventitial space formed the lateral wall of the aneurysm (Fig 3). The inner layer of the aneurysm dome was covered with the fresh thin clots in the acute stage, and it was fully endothelialized in the chronic stage; the latter was clearly demonstrated at SEM (Fig 3).

Statistical analysis

In the comparison based on the sizes of intimal entry zone, the likelihood of aneurysm formation was significantly greater in group I-B than in I-A and I-D ($P < .01$). The lesions in the I-D were more likely cause occlusion in the artery those with a shorter entry zone ($P < .01$). Longitudinal incisions had no obvious morphologic differences related to length.

Discussion

Dissection can occur in any artery throughout the body. Many points of uncertainty or controversy with respect to cause, pathogenesis, and treatment strategy remain. To address some of these issues, particularly in cases of aortic dissection, various experimental models have been used. Wilens et al (10) ligated several feeding branches to the aorta in mongrel dogs, whereas Takeoka (11) infiltrated mitomycin C into the media of the canine aorta. In both studies, only medial edematous change developed, and spontaneous dissection did not. Aortic dissection also failed to develop in dogs with renal hypertension (11). Takeoka created a traumatic dissection model with surgical methods and succeeded in producing an aortic lesion with a pseudolumen. However, to our knowledge, surgical lesion creation has not been used to produce carotid dissection until now, and ours is the first report of an experimental model of carotid artery dissection.

In our experimental model, artificial dissection was produced physically, with the intention to mimic traumatic dissection. This model had angiographic and histopathologic changes similar to those in clinical cases (1, 5–8, 12, 13). Regarding the initial findings after the artificial dissection was produced, angiograms depicted either a double shadow (pseudolumen) or stenosis in the affected artery due to compression from the subadventitial hematoma in all cases. In some lesions with a pseudolumen, a dissecting aneurysm subsequently developed. Some arteries with focal occlusion recanalized, and stenosis spontaneously improved. Our findings indicated that the size of intimal entry zone strongly affected subsequent morphologic differences. These results may serve as important clues to the mechanism of dissection, particularly aneurysm formation and dissecting occlusion. To induce morphologic changes characteristic of dissection, a sufficiently large entry zone is needed. Most arteries with a short longitudinal incision (II-A) or a small elliptical defect (I-A) eventually

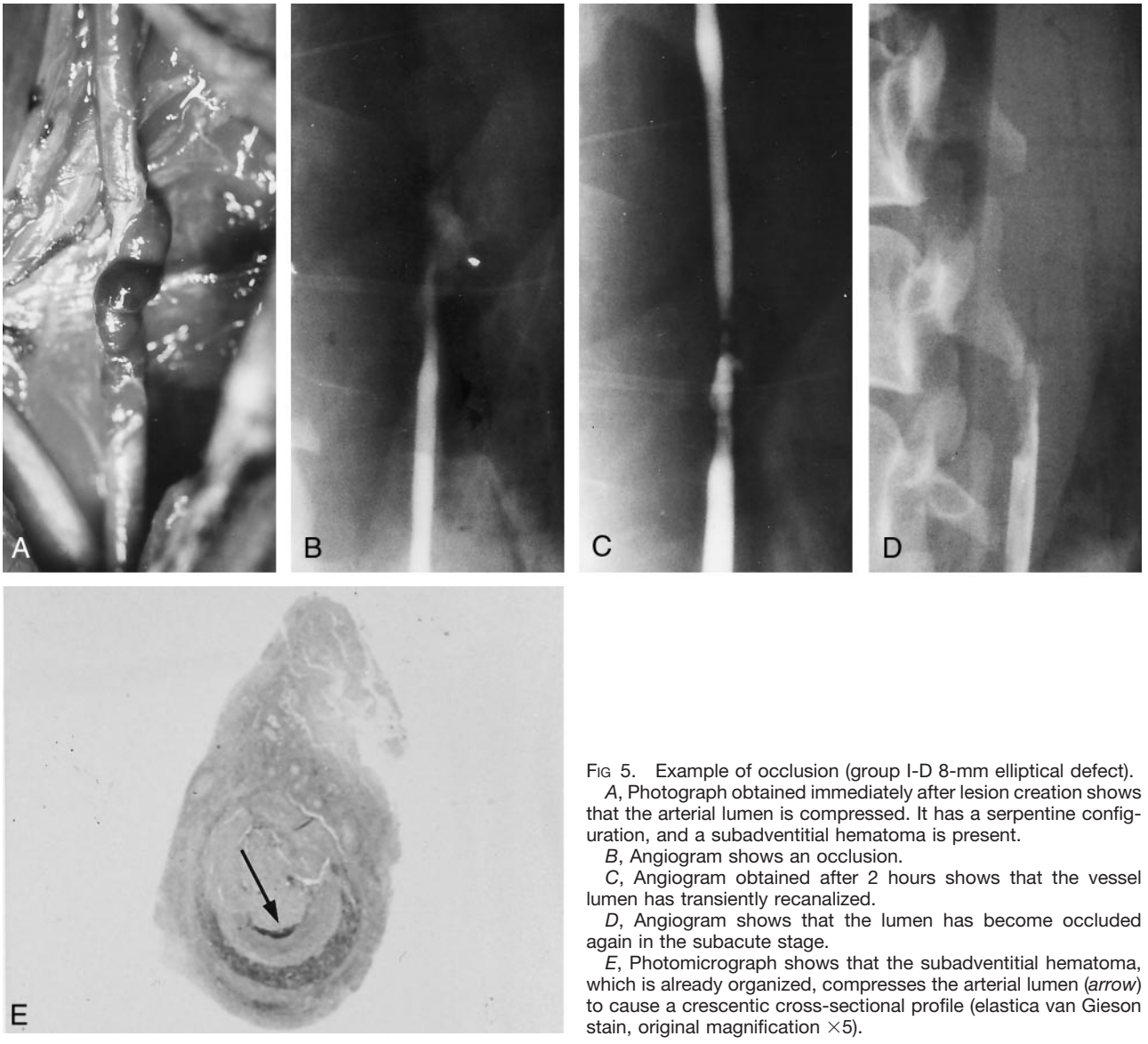

FIG 5. Example of occlusion (group I-D 8-mm elliptical defect).

A, Photograph obtained immediately after lesion creation shows that the arterial lumen is compressed. It has a serpentine configuration, and a subadventitial hematoma is present.

B, Angiogram shows an occlusion.

C, Angiogram obtained after 2 hours shows that the vessel lumen has transiently recanalized.

D, Angiogram shows that the lumen has become occluded again in the subacute stage.

E, Photomicrograph shows that the subadventitial hematoma, which is already organized, compresses the arterial lumen (*arrow*) to cause a crescentic cross-sectional profile (elastica van Gieson stain, original magnification ×5).

FIG 6. Diagrams show hypothetical schemes of aneurysm formation (*left*) and persistent stenosis (*right*).

Left, Hemodynamic stress from vortex flow inside the cavity may cause external protrusion of the adventitia, which results in a saccular aneurysm.

Right, A large entry zone can produce a massive, widespread subadventitial hematoma of sufficient size to compress the true lumen and result in abrupt occlusion. When the hematoma is large, the artery is likely to remain thrombosed.

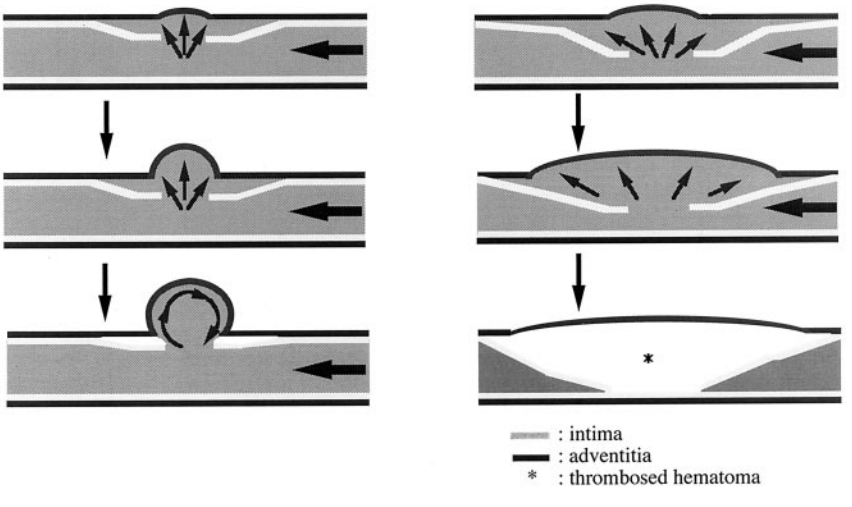

normalized. Such spontaneous healing due to shrinkage of the dissected pseudolumen might be possible because of the limited extent and thickness of the subadventitial hematoma, which reflects the low and ineffective influx pressure. In addition, a medium entry zone with a 4- or 6-mm-long elliptical orifice (I-B, I-C) frequently resulted in saccular aneurysms corresponding to the site of intimal entry zone. This observation suggests that the size of entry zone is important for delayed aneurysm formation. Some reports describe the mechanism of saccular aneurysm dilation as hemodynamic stress that disrupts the intima, internal elastic lamina, and media at the entry point of arterial dissection (14). We speculate that an unthrombosed dissected cavity can persist at the initial stage with a suitable balance of blood inflow and outflow at the orifice (15–20). At first, a subadventitial hematoma may be only a diverticulum, but hemodynamic stress from vortex flow inside the cavity may cause further external protrusion of the adventitia, producing a saccular aneurysm (Fig 6).

Histopathologically, the dome of the aneurysm consisted of a layer of adventitia lined by newly formed endothelium. This absence of a media layer that contains smooth muscle is similar to the characteristics of intracranial aneurysms (21–25). Thus, the histopathologic and macroscopic features of this experimental aneurysm more closely approximate those of clinically encountered aneurysms than those of a previous model involving a sutured venous pouch (26).

A large entry zone can permit formation of a massive, extensive subadventitial hematoma sufficient to compress the true lumen, resulting in an abrupt occlusion (Fig 6). When the hematoma is particularly large, the artery is expected to remain thrombosed. However, some lesions with initial occlusion recanalized during the early period, probably because of vascular remodeling or distal migration of clots. The migration phenomenon may explain clinical episodes of distal intracranial embolism that are observed in the acute stage of cervical arterial dissection (7). Thus, the most important factor that determines the morphologic features and their course after dissection may be the extent of the intimal entry zone, irrespective of layers dissected.

We were able to simulate some clinical features of arterial dissection in our model, but, in some respects, the model notably differed from clinical dissections. First, intracranial vertebral artery dissection frequently has fusiform dilatation (9, 27, 28). Histopathologically, intracranial vertebral dissecting aneurysms have widespread disruption of the internal elastic lamina within the wall of the fusiform aneurysm (29–32). In a previous study of experimental saccular aneurysms, extensive infusion of elastase caused widespread degeneration of the elastic lamina and resulted in fusiform aneurysmal dilatation, not saccular aneurysm formation. Localized small defects in the elastica should cause a saccular aneurysm, whereas extensive disruption of the elastic layers should cause a fusiform aneurysm (14, 21, 23–25, 33). In our experiment, however, no fusiform aneurysms were observed. Instead, an extensive intimal entry zone (group I-D) resulted in arterial occlusion. Although the structure of the intracranial vessel wall differs from that of the CCA, additional factors not present in our model apparently result in fusiform aneurysms (32, 34).

Second, in our model, dissecting aneurysms never had a reentry zone. The concept of entry and reentry has been generally accepted, not only for aortic dissection but also for carotid and vertebral lesions. Before the present experiments, we created entry and reentry zones by making two intimal entry zones in some animals, but the result was simply two aneurysms, one at each site of intimal entry zone. While no reentry occurred beyond the intimal entry zone in our cases, such situations have been described in previous reports (30, 31). We believe that the saccular aneurysms located at the dissection site in our model had no reentry and that they were morphologically similar to saccular aneurysms with a single orifice. However, these issues must be resolved with further experimental studies.

Although our model is one of traumatic dissection, a model of spontaneous dissection might be created by using biochemical or molecular methods. Such further investigation will improve our understanding of aneurysm formation in a variety of circumstances. The contribution of hemodynamic stress is an important factor to assess in such experimental systems.

Conclusion

Morphologic changes after experimental carotid dissection are affected by the size of the intimal entry zone. Very small dissections result in spontaneous healing, while large intimal entry zones cause stenotic lesions. However, a medium entry zone (4–6 mm) may induce aneurysm formation. The different features of dissection may be caused by characteristics of flow into the subadventitial cavity and by thrombogenesis. Consideration of intimal entry zone size is important for understanding the features of traumatic dissection in extracranial arteries, and studies of additional factors are needed to elucidate the mechanisms of idiopathic and hypertensive intracranial arterial dissection.

References

1. Anson J, Crowell RM. **Cervicocranial arterial dissection.** *Neurosurgery* 1991;29:89–96
2. Cloft HJ, Jensen ME, Kallmes DF, et al. **Arterial dissections complicating cerebral angiography and cerebrovascular interventions.** *AJNR Am J Neuroradiol* 2000;21:541–545
3. Hinse P, Thie A, Lachenmayer L. **Dissection of the extracranial vertebral artery: report of four cases and review of the literature.** *J Neurol Neurosurg Psychiatry* 1991;54:863–869
4. Miyachi S, Okamura K, Watanabe M, et al. **Cerebellar stroke due to vertebral artery occlusion after cervical spine trauma.** *Spine* 1994;19:83–88
5. Mokri B, Piepgras G, Houser W. **Traumatic dissection of the extracranial internal carotid artery.** *J Neurosurg* 1988;68:189–197
6. Okada Y, Shima T, Nishida M, et al. **Traumatic dissection of the**

common carotid artery after blunt injury to the neck. *Surg Neurol* 1999;51:513–520
7. Pozzati E, Giuliani G, Poppi M, et al. **Blunt traumatic carotid dissection with delayed symptoms.** *Stroke* 1989;20:412–416
8. Stringer WL, Kelly DL. **Traumatic dissection of the extracranial internal carotid artery.** *Neurosurgery* 1980;6:123–130
9. Kitanaka C, Tanaki J, Kuwahara M, et al. **Nonsurgical treatment of unruptured intracranial vertebral artery dissection with serial follow-up angiography.** *J Neurosurg* 1994;80:667–674
10. Wilens SL, Malcolm JA, Vazquez JM. **Experimental infarction (medical necrosis) of the dog's aorta.** *Am J Pathol* 1965;47:695–711
11. Takeoka T. **An experimental study on dissecting aortic aneurysm [Japanese].** *J Jpn Asso Thorac Surg* 1984;32:174–186
12. Farrell MA, Gilbert JJ, Kaufmann JC. **Fatal intracranial arterial dissection: clinical pathological correlation.** *J Neurol Neurosurg Psychiatry* 1985;48:111–121
13. Miyachi S, Ishiguchi T, Taniguchi K, et al. **Endovascular stenting of a traumatic dissecting aneurysm of the extracranial internal carotid artery.** *Neurol Med Chir (Tokyo)* 1997;37:270–274
14. Takagi M, Hirata K, Fujitsu K, et al. **Unusual angiographic changes in a dissecting aneurysm of the basilar artery: case report.** *Neurosurgery* 1994;34:356–358
15. Burleson AC, Strother CM, Turitto VT. **Computer modeling of intracranial saccular and lateral aneurysms for the study of their hemodynamics.** *Neurosurgery* 1995;37:774–784
16. Gonzales CF, Cho YI, Ortega HV, et al. **Intracranial aneurysms: flow analysis of their origin and progression.** *AJNR Am J Neuroradiol* 1992;13:181–188
17. Graves VB, Strother CM, Partington CR, et al. **Flow dynamics of lateral carotid artery aneurysms and their effects on coils and balloons: an experimental study in dogs.** *AJNR Am J Neuroradiol* 1992;13:189–196
18. Liepsch DW, Steiger HJ, Poll A, et al. **Hemodynamic stress in lateral saccular aneurysms.** *Biorheology* 1987;24:689–710
19. Perktold K, Gruber K, Kenner T, et al. **Calculation of pulsatile flow and particle paths in an aneurysm model.** *Basic Res Cardiol* 1984; 79:253–261
20. Strother CM, Graves VB, Rappe A. **Aneurysm hemodynamics: an experimental study.** *AJNR Am J Neuroradiol* 1992;13:1089–1095
21. Anidjar S, Salzmann JL, Gentric D, et al. **Elastase-induced experimental aneurysms in rats.** *Circulation* 1990;82:973–981
22. Cawley CM, Dawson RC, Shengelaia G, et al. **Arterial saccular aneurysm model in the rabbit.** *AJNR Am J Neuroradiol* 1996;17: 1761–1766
23. Halpern VJ, Nackman GB, Gandhi RH, et al. **The elastase infusion model of experimental aortic aneurysms: synchrony of induction of endogenous proteinases with matrix destruction and inflammatory cell response.** *J Vasc Surg* 1994;20:51–60
24. Kim C, Cervos-Navarro J, Kikuchi H, et al. **Degenerative changes in the internal elastic lamina relating to the development of saccular cerebral aneurysms in rats.** *Acta Neurochir (Wien)* 1993;121: 76–81
25. Miskolczi L, Guterman LR, Flaherty JD, et al. **Saccular aneurysm induction by elastase digestion of the arterial wall: a new animal model.** *Neurosurgery* 1998;43:595–601
26. Varsos V, Heros RC, Debrun G, et al. **Construction of experimental "giant" aneurysms.** *Surg Neurol* 1984;22:17–20
27. Shimoji T, Bando K, Nakajima K, et al. **Dissecting aneurysm of the vertebral artery: report of seven cases and angiographic findings.** *J Neurosurg* 1984;61:1038–1046
28. Yasui T, Komiyama M, Nishikawa M, et al. **Fusiform vertebral artery aneurysms as a cause of dissecting aneurysms: report of two autopsy cases and a review of the literature.** *J Neurosurg* 1999;91: 139–144
29. Endo S, Nishijima M, Nomura H, et al. **A pathological study of intracranial posterior circulation dissecting aneurysms with subarachnoid hemorrhage: report of three autopsied cases and review of the literature.** *Neurosurgery* 1993;33:732–738
30. Endo S, Takaba M, Ogiichi T, et al. **Pathological study of intracranial artery dissection with subarachnoid hemorrhage [Japanese].** *Surg Cereb Stroke (Jpn)* 1997;25:169–176
31. Mizutani T, Miki Y, Kojima H, et al. **Proposed classification of nonatherosclerotic cerebral fusiform and dissecting aneurysm.** *Neurosurgery* 1999;45:253–260
32. Sasaki O, Ogawa H, Koike T, et al. **A clinicopathological study of dissecting aneurysms of the intracranial vertebral artery.** *J Neurosurg* 1991;75:874–882
33. Ammirati M, Cozzens J, Eller T, et al. **Technique of experimental aneurysm formation in the rat common carotid artery using the milliwatt carbon dioxide laser and the adventitia patch model.** *Neurosurgery* 1986;19:732–734
34. Wilkinson IMS: **The vertebral artery: extracranial and intracranial structure.** *Arch Neurol* 1972;27:392–396